The Dynamic Response of SPWM vs. SVPWM Synchronverter

KHALED A. MAHAFZAH
Depart. of Electrical Eng.
Al-Ahliyya Amman University
Amman-19328
JORDAN

HANA'A A. RABAB'AH
Depart. of Electrical Eng.
Al-Ahliyya Amman University
Amman-19328
JORDAN

ABDULLAH AL-ODIENAT
Electrical Engineering Depart.
Mutah University
Karak-61710
JORDAN

MOHAMMAD AL-MOMANI
Protection & maintenance
section
NEPCO
Amman
JORDAN

KHALED AL-MAITAH
Technical Department
Electricity Distribution Co.
EDCO
Amman
JORDAN

AMNEH AL-MBAIDEEN
Electrical Engineering Depart.
Mutah University
Karak-61710
JORDAN

Abstract: - This paper explores the use of Space Vector Pulse Width Modulation (SVPWM) instead of Sinusoidal Pulse Width Modulation (SPWM) to evaluate dynamic response of the synchronous inverter (synchronverter). The paper presents a comprehensive comparison between the SVPWM and SPWM for the dynamic response of synchronverter. This comparison aspects contain: the grid frequency, the active and reactive power, line current and its THD and rate of change of frequency (RoCoF) in case of using both modulation techniques. Despite the complexity of using SVPWM, it has several advantages over SPWM. With the increased penetration of renewable energy sources in power systems, the system inertia is reduced, and the frequency deviations becomes greater and faster. The results of this paper show that SVPWM contributes to reducing the rate of change of frequency (RoCoF) which enhances the system inertia. The results show a more stable behavior of SVPWM than the SPWM. Moreover, SVPWM reduces the total harmonics distortion (THD) of the current by 7% as compared to SPWM. Furthermore, the use of SVPWM reduces the complexity and the cost of the used filter. Matlab/Simulink is used for results validation.

Key-Words: - Dynamic Response, Frequency Stability, Inertia, Pulse Width Modulation (PWM), Space Vector PWM (SVPWM), Synchronous Inverter (Synchronverter), Total Harmonics Distortion (THD).

Received: April 20, 2021. Revised: April 18, 2022. Accepted: May 19, 2022. Published: June 17, 2022.

1 Introduction

Integration of renewable energy resources in modern power systems increases the dependency on the inverter-based generators. Therefore, many concerns appear around frequency stability and power quality issues [1]. Inverter-based generators are integrated with the grid, but they are not able to provide inertia to the system. One of inertia issues related to the inverter usage is the low-frequency oscillations. They are mainly generated due to the moment of inertia of the conventional synchronous generators following some events in the system [2].

The lack of low-frequency oscillation dampers may lead to system collapse [3]. The synchronverter is proposed to mimic synchronous generator (SG) performance in the inverter controller [4]. Synchronverter can be connected and operated in parallel, sharing the real and reactive power. It can also be operated in islanding mode of microgrids [4]-[5]. The grid-connected synchronverter is shown in Figure 1 [4]. It consists of two main parts: the power part and the control part, containing two control loops for real and reactive power instead of voltage and current loops.

The grid connected inverter is unavoidably implicating harmonic elements linked with switching frequency [7]. To reduce the harmonic components normally a simple L filter is used. However, the drawback of this system is the increased size of the filter. Moreover, the system response becomes lower which increases the probability of the under-voltage events across the grid. Also, the L filter needs high frequency commutation which increases the switching losses in the inverters [8-9].

To overcome the L filter disadvantages, an LCL filter is presented. This filter has a third order low-pass filter characteristic. At smaller capacity of the LCL, it can achieve the same attenuation of L filter. Therefore, reduces the manufacturing costs [9]-[12]. Synchronverter is connected to the grid through an LCL filter. As depicted from Figure 1, the inductance Lf1 plays the role of the SG stator windings. The filter capacitance Cf ensures the elimination of the ripple from the output voltage. Therefore, the behavior of SG is accomplished.

The high-speed response of the inverter controller better damps low-frequency oscillations than the exciter controller. The harmonics produced by the inverter can be eliminated by using a suitable modulation technique alongside with an external filter [5]. In literature, synchronverter modeling and simulation have been addressed from different aspects. Some researchers investigated its topology [4], [6]. They focused on their works on the emulation of SG to preserve its features in synchronverter. Other researchers focused on the control parts of the synchronverter and proposed different control strategies to enhance its response.

A Pulse Width Modulation (PWM) technique is required to achieve a variable output voltage of the inverter; by varying the inverter gain within a switching sequence accomplished within a PWM technique. Numerous PWM methods are illustrated in the literature, e.g., Sinusoidal Pulse Width Modulation (SPWM), Space Vector Pulse Width Modulation (SVPWM), Hysteresis Band Pulse Width Modulation (HBPWM). They are used to: i) tackle the current harmonics distortion, ii) reduce the switching losses in the inverter and iii) implement a robust control [13], [14]. However, the literature addresses that SVPWM has more different merits over other modulation techniques. In [15], [16] a comparison between SPWM and SVPWM techniques (they are the most common modulation methods) is presented; the results confirm that SVPWM is more efficient in term of THD level and switching losses reduction.

Recent literature presents many algorithms from a control point of view [17], [18]. An adaptive control strategy is proposed in [19] for the interfacing of converter-based resources using synchronverters. In this work, many types of energy resources are connected to a DC bus, the rotor equation is used in its control loop to mimic synchronous machine characteristics. The dynamic response of the system and the impact of the controller parameters are investigated. The results show that the damping ratio decreases when the virtual moment of inertia is increased. Moreover, the system dynamic performance during load variation.

Reference [18] presents an improved control algorithm based on fuzzy logic. The proposed algorithm is aimed at improving the droop coefficient. The authors of [19] and [20] discussed the importance of the power system inertia. Synchronverters are used to enhance the system stability. An interactive control loop in [21] is designed to give more freedom in the system parameters selection to enhance the system dynamics without affecting its frequency droop characteristics. A new technique is proposed in [22] to obtain a small signal model based on Phasor Measuring Units (PMUs). Reference [23] presents an optimization technique for the synchronverter operational parameters. The system is modeled using the dynamic phasor principle. Furthermore, a small-signal analysis is used to assess its transient behavior.

A synchronous inverter (Inverter with virtual inertia) is one of the promising technologies that is aimed at meeting the challenges facing modern power systems. After a comprehensive literature review, the authors of this work found that the topic of Space Vector Pulse Width Modulation (SVPWM) with synchronous inverter is not addressed from all its aspects. Therefore, the authors believe that this work presents a very important material for the interested researchers. To the best of authors' knowledge, this paper is the first to recommend using the SVPWM with synchronverter in power systems. In this work, the dynamic response of a grid connected SVPWM synchronverter is assessed in terms of frequency, Rate of Change of frequency (RoCoF), active and reactive power, line current, and its Total Harmonics Distortion (THD). Results of the paper shows that SVPWM synchronverter outperforms SPWM synchronverter. The simulation results show that the dynamic response of the synchronverter is enhanced when using SVPWM instead of SPWM. Moreover, when the SVPWM synchronverter is used, the THD of the line current of is lower by 7% than the THD of the SPWM synchronverter. Results are obtained using MATLAB/Simulink.

The paper is organized as follows: the introduction is presented in section 1. A brief discussion of the synchronverter model is summarized in Section 2; Section 3 briefly presents the SVPWM technique for the synchronverter. Section 4 prepares the simulation model. An extended and deep Discussion of the simulation results is presented in Section 5. Section 6 evaluates the performance of the SVPWM synchronverter. Finally, Section 7 is the conclusion.

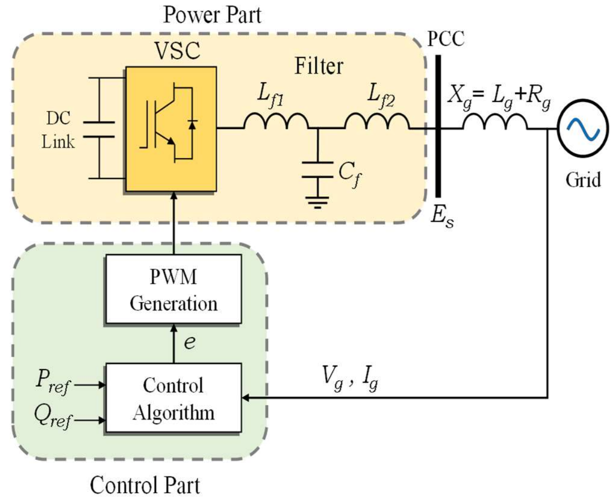

Figure 1. Main blocks of synchronous inverter presented in [4].

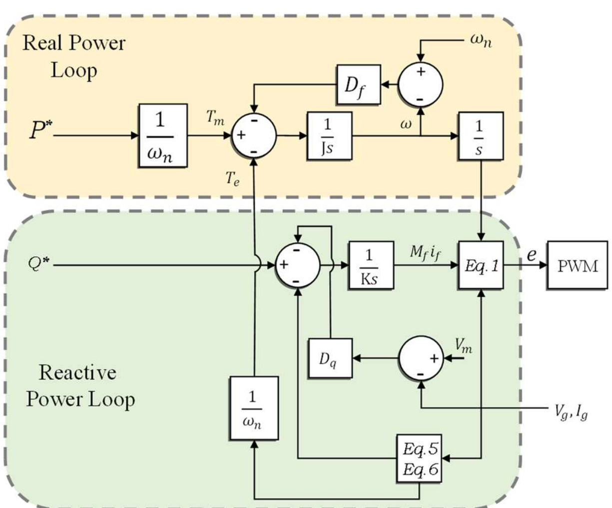

Figure 2. Real and reactive power control loops of a synchronous inverter [4].

2 Modelling of Synchronverter

The Synchronverter is basically employed to emulate the behavior of the SG. It is a DC/AC converter (inverter) used to generate three phase AC power from DC power supply. As seen in Figure 1, three legs of the conventional inverter are modulated by Pulse Width Modulation (PWM) connected to three LCL filters to minimize the voltage and current ripple. The filter capacitors with the left Inductances of Figure 1 are the power part of the synchronverter. The synchronverter behaves like a SG in parallel with the capacitors, voltage ripple is ignored. The synchronverter electronic part is represented by a real and reactive power control loop, as shown in Figure 2.

2.1 Power Part

The terminal voltages of the synchronverter are regulated using three capacitors as seen in Figure 1. The inductor L_{f1} simulates the stator winding of the SG. The Electro-Motive Force (back EMF) is virtually the SG rotor movement. The DC bus is acting as an adjustable DC current source to feed the virtual rotor. Virtually, it can be assumed that the rotor movement of the SG is denoted by three EMFs (e_a, e_b and e_c). The generated induced voltage is reduced to:

$$e = \dot{\theta} M_f i_f \widetilde{\sin}\,\theta, \tag{1}$$

2.2 Control Part

The real and reactive power generated from synchronverter can be defined as:

$$P = \langle i, e \rangle \tag{2}$$

$$Q = \langle i, e_q \rangle \tag{3}$$

Where, e_q has the same amplitude as e with a phase difference of $\pi/2$; i.e.:

$$e_q = \dot{\theta} M_f i_f \widetilde{\sin}\left(\theta - \frac{\pi}{2}\right) = -\dot{\theta} M_f i_f \widetilde{\cos}\,\theta \tag{4}$$

Then, the real and reactive power are:

$$P = \dot{\theta} M_f i_f \langle i, \widetilde{\sin}\,\theta \rangle \tag{5}$$

$$Q = -\dot{\theta} M_f i_f \langle i, \widetilde{\cos}\,\theta \rangle \tag{6}$$

2.3 The Mechanical Part representation of SG

The dynamic equation of the SG is given by:

$$J\ddot{\theta} = T_m - T_e - D_p\dot{\theta} \tag{7}$$

Where J is the moment of inertia of the rotating parts with the rotor, Tm is the mechanical torque, T_e is the electromagnetic torque, and D_p is the damping factor. T_e can be obtained from the stored energy in the magnetic field of the machine as the following equation:

$$T_e = -M_f i_f \langle i, \frac{\partial}{\partial\theta} \widetilde{\cos}\,\theta \rangle = M_f i_f \langle i, \widetilde{\sin}\,\theta \rangle \tag{8}$$

To obtain the stability of the synchronverter, the SG modeling is used to regulate the active and reactive power loops. Hence, (7) can be rewritten to represent the power loop control of the synchronverter as follow

$$\ddot{\theta} = \frac{1}{J}(T_m - T_e - D_p\dot{\theta}) \quad (9)$$

where the mechanical torque Tm is the control input and T_e depends on the current i and Θ as illustrated in (8).

2.4 Active and Reactive Control Loop

Power control loops maintain the synchronverter working on the same mode as such to emulate the SG dynamics properly. As illustrated in Figure 2, the active power loop contains cascaded control loops, inner and outer with the consideration of their bandwidth to achieve the proper steady-state stability. Eqs. (5) and (6) are both used to regulate and model the SG active and reactive power control. The control loops regulate the active and reactive power to track their reference values (Q_{ref}, P_{ref}). The upper control scheme (active power loop) includes two cascaded control loops. The inner is the frequency regulation (with a gain D_f) and the outer is the torque loop. D_f represents the mechanical friction coefficient (frequency drooping coefficient), which is the rate of change ratio between the torque and the frequency.

The amount of active power delivered by the SG varies with the grid frequency variations, which is maintained by frequency droop control. In synchronverter, frequency droop regulation is obtained by multiplying the difference between the reference (nominal) and the synchronverter frequencies with the frequency drooping coefficient D_f. The resulting signal is summed up with the torque signal. The mechanical torque is obtained by dividing the reference active power by the nominal frequency. Then, the difference between T_m and the electrical torque T_e is calculated from (8) depending on the grid current I_g, which completes the active power control scheme.

In the reactive power loop, the error between the reference reactive power (Q_{ref}) and the reactive power (Q) is calculated from (6). The resulting tracking error between the grid feedback voltage V_g and the reference voltage V_m is multiplied with the Drooping Coefficient D_q, which is added to the power tracking error. The net resulting error is fed to an integrator with a gain of $\frac{1}{k}$ to regulate the excitation field $M_f i_f$. The reactive power control loop contains inner and outer loops, voltage, and reactive power loop respectively. To achieve the proper steady state-stability the bandwidth of the inner loop is set higher than the outer loop. The interaction between active and reactive power loops generates the induced voltage as represented in (1) which is used to generate the proper switching sequences of the synchronverter using SVPWM.

3 Space Vector Pulse Width Modulation

The increasing demand for inverters comes from their ability to control the speed of variable speed drives in the industry [24]. The SPWM can control the magnitude and frequency of the inverter's output voltage [25] - [26]. In SPWM the switching sequence is generated by comparing a triangular carrier with three- phase reference modulating signals. While in case of SVPWM a reference voltage vector is used instead of the three- phase modulating signals [27]. SVPWM shows a better performance compared to SPWM; it generates less harmonic distortion and employs efficient DC bus voltage [28], [29].

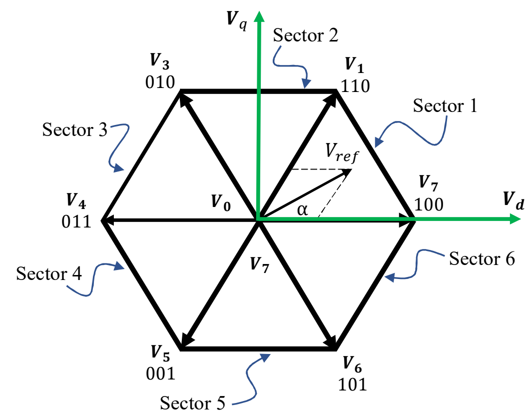

Figure 3. The Principle of SVPWM, the reference voltage rotates within a switching cycle, Ts.

Alternatively, SVPWM is used to generate the inverter switching pulses. It offers a degree of freedom for vector placement during a complete switching cycle which reduces the output current's Total Harmonic Distortion (THD) [30]. The main principle of SVPWM is based on replacing three vectors with only two orthogonal vectors. The three-line voltages are transformed from ABC to d-q frame using Park's transformation [31]-[33]. The reference vector magnitude, see Figure 3, can be estimated by:

$$V_{ref} = \sqrt{V_d{}^2 + V_q{}^2} \quad (10)$$

$$\alpha = \tan^{-1}\left(\frac{V_q}{V_d}\right), \quad (n-1) < \alpha < n\frac{\pi}{3} \quad (11)$$

and,

$$V_d = \frac{2}{3}(V_{an} - V_{bn} - V_{cn}) \quad (12)$$

$$V_d = \frac{2}{3}(V_{an} - V_{bn} - V_{cn}) \quad (13)$$

where, for continuous SVPWM operation, n is an integer from one up to six, V_{an}, V_{bn}, V_{cn} are phase voltages of the inverter.

The reference vector V_{ref} rotates within a complete duty cycle, forming a hexagon, as illustrated in Figure 3. Assume the switching cycle Ts is divided into three time slots, T1, T2, and T3, such that:

$$T_s = T_1 + T_2 + T_3 \tag{14}$$

These time slots are determined carefully to avoid any crossover between switches during the inverter operation. The time slots are changed according to the sector number (n). Thus:

$$T_1 = \frac{\sqrt{3}\, T_s V_{ref}}{V_{dc}} \sin\left(\frac{\pi}{3} - \alpha + \frac{n-1}{3}\pi\right) \tag{15}$$

$$T_2 = \frac{\sqrt{3}\, T_s V_{ref}}{V_{dc}} \sin\left(\alpha - \frac{n-1}{3}\pi\right) \tag{16}$$

where V_{dc} represents the DC input voltage of the inverter.

$$T_3 = T_s - T_1 - T_2 \tag{17}$$

Table 1 summarizes each switching cycle's per sector [31]- [32].

Table 1. Conventional Inverter Switching Times per Sector per Ts.

Sector (n)	Upper Switches	Lower Switches
1	$S_1 = T_1 + T_2 + T_3/2$ $S_3 = T_2 + T_3/2$ $S_5 = T_3/2$	$S_4 = T_3/2$ $S_6 = T_6 + T_3/2$ $S_2 = T_1 + T_2 + T_3/2$
2	$S_1 = T_1 + T_3/2$ $S_3 = T_1 + T_2 + T_3/2$ $S_5 = T_3/2$	$S_4 = T_4 + T_3/2$ $S_6 = T_3/2$ $S_2 = T_1 + T_2 + T_3/2$
3	$S_1 = T_3/2$ $S_3 = T_1 + T_2 + T_3/2$ $S_5 = T_2 + T_3/2$	$S_4 = T_1 + T_2 + T_3/2$ $S_6 = T_3/2$ $S_2 = T_1 + T_3/2$
4	$S_1 = T_3/2$ $S_3 = T_1 + T_3/2$ $S_5 = T_1 + T_2 + T_3/2$	$S_4 = T_1 + T_2 + T_3/2$ $S_6 = T_2 + T_3/2$ $S_2 = T_3/2$
5	$S_1 = T_2 + T_3/2$ $S_3 = T_3/2$ $S_5 = T_1 + T_2 + T_3/2$	$S_4 = T_1 + T_3/2$ $S_6 = T_1 + T_2 + T_3/2$ $S_2 = T_3/2$
6	$S_1 = T_1 + T_2 + T_3/2$ $S_3 = T_3/2$ $S_5 = T_1 + T_3/2$	$S_4 = T_3/2$ $S_6 = T_1 + T_2 + T_3/2$ $S_2 = T_2 + T_3/2$

4 Model Preparation

The synchronverter is presented with different inertia emulation techniques, control loops, self-synchronizing techniques, and applications [34]. The simulation model used in this paper is proposed in [4]. A brief description and values of all parameters are shown in Table 2. The results are achieved using MATLAB R2020a. The selected solver is an ordinary differential equation ode23tb with a relative tolerance of 10−3 and a maximum step size of 0.2 ms. Before simulating with SVPWM, the SPWM is used to modulate the synchronverter. The key results are compared to the presented in [4] to check the validity of the model.

Table 2. Parameters of The Simulated Model.

Parameter	Value	Description
P_o	100W	Rated Power
V_{dc}	42V	DC link voltage
F	50Hz	Grid frequency
f_s	15KHz	The switching frequency
R_g	0.135 Ω	Grid resistance
L_g	0.45mH	Grid inductance
C_f	22μF	Filter capacitance
R_p	1000	Parallel ESR
D_q	117.88	The voltage drooping coefficient
D_p	0.2026	The mechanical friction coefficient
τ_v	0.002s	Voltage loop time-constant
τ_f	0.002s	Frequency loop time-constant
P^*	80W	The reference real power
Q^*	60VAR	The reference reactive power

5 Simulation Results and Discussion

In this section, a comprehensive comparison between SPWM and SVPWM is conducted. The effectiveness of the proposed modulation method on the power quality and system dynamic behavior is proved. A comparison between SPWM and SVPWM in term of grid frequency, output power and output current with its harmonics contents is presented in the following subsections.

5.1 The Grid Frequency

The conventional generators have a rotating mass of inertia stores energy in the mechanical rotating part. Conversely, an inverter-based generator does not provide any inertial response to the grid. The energy stored in the rotating part of the generator is crucial for stability. Thus, synchronverter should mimic the synchronous machine perfectly.

The grid frequency response reflects the state of system stability or system inertia. One of the main applications of the synchronverter in the power system is to increase the system inertia to handle different system events without any stability problems. Furthermore, the synchronverter can emulate the synchronous machine at distributed generation level. In this section, the frequency response of the synchronverter for different power system events are studied using SPWM and SVPWM to prove the benefits of the SVPWM over SPWM.

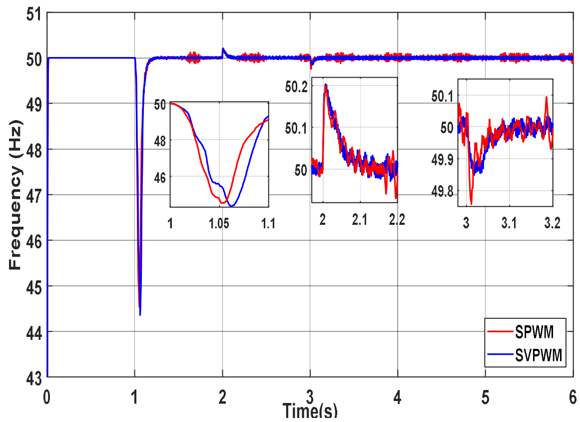

Figure 4. The grid frequency using both modulation methods for synchronverter.

Figure 4 (with zoom-in windows in the figure) shows the frequency response of the synchronverter under three loading conditions: connected to the grid, increasing the load, decreasing the load. For the condition when the synchronverter is connected to the primary grid, the system frequency drops to about 45 Hz for both modulation methods. It is noted that the SPWM has faster response than the SVPWM, which confirms that the inertia is better in case of the SVPWM than SPWM. The ripple around the system frequency, which refers to the damping performance of the synchronous generators (hunting), disappears for the SVPWM method; furthermore, the SVPWM method can mimic the damping performance of the SG much better than the SPWM method. From the same figure, multi non-triggered oscillations appears in SPWM at 1.6 s, 2.4 s, 3.3 s, 4 s, 4.6 s, and 5.2 s SPWM is less stable than the SVPWM.

5.2 Active and Reactive Power

The output power indicates the synchronverter performance and its ability to mimic an SG. In case of steady-state stability, the amount of energy that the synchronverter can provide to the grid in sudden load-up events is proportional to the inverter size. The slope of the synchronverter output power for sudden load-down events is calculated as a rate of change of power to estimate the system inertia. The low system inertia could jeopardize the system stability during contingency. The high penetration of renewable energy resources in power system reduces the total system inertia.

Both of SPWM and SVPWM introduce ripple in the output active and reactive power, as shown in Figures 5, 6. Figure 5 shows the active power delivered by the synchronverters. The output active power of the SPWM has a constant ripple, while SVPWM synchronverter has variable ripple magnitude. On the other hand, the reactive power, depicted in Figure 6, has a ripple of low-frequency oscillation, while the magnitude of the ripple varies in a uniform matter. The response of the SVPWM is faster than SPWM in term of injecting reactive power into the system, which should enhance the output voltage of the synchronverter.

It is important to explain there is a big step in the active power of the inverter at synchronizing time, see Figure 5.a. This is related to the load angle of the phase locked loop. In future work, the design of both PLL and self-synchronizing methodology will be presented.

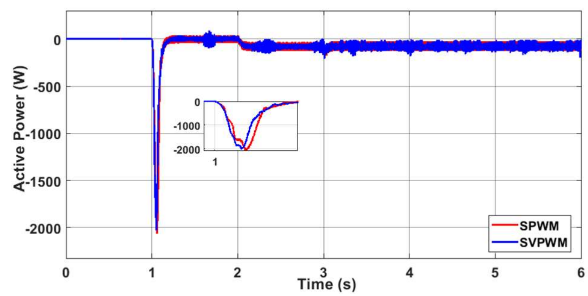

Figure 5: The active power of the synchronverter using two modulation methods.

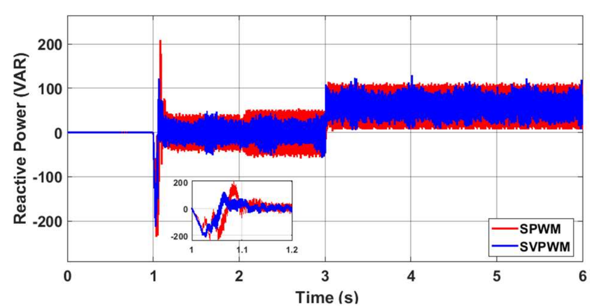

Figure 6: The reactive power of the synchronverter using two modulation methods.

5.3 Line Current and THD

The other key benefit of the synchronverter is the ability to control the short circuit level at the connecting point. The deficient short circuit level at any point in the system makes it difficult for the protection system to sense a fault. A very high short circuit level may lead to component failure. The short circuit current level should be carefully designed and controlled for the component capability and the protection system sensitivity.

The short circuit level at any electrical point can be estimated based on the rate of change of the output voltage with respect to the rate of change of current at any unexpected fault. Because the output voltage mainly depends on the system, the output current of the synchronverter plays a significant role in controlling the short circuit level at the connecting point. The switching nature of the power converters deteriorates the power quality. One of the main indications to present the power quality problems is the harmonic in the current. The output current of the producer/end-user should have pure sine wave at the grid frequency and constant magnitude.

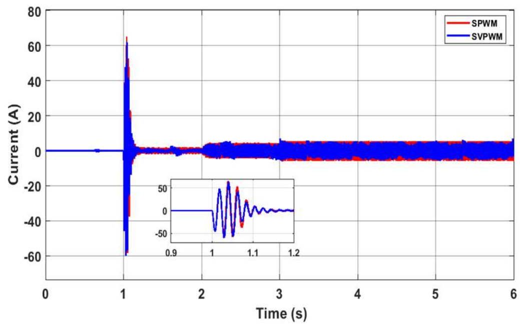

Figure 7. The synchronverter output current using two modulation methods under different loading conditions.

Figure 7 depicts the output current for both PWM methods. It is observed that the sudden change in the input current due to the synchronverter switching of the synchronverter reached about 60 A. At t = 2 s, the output current increased due to the step-change in power demand by 80W. At t=3 s, the output current enters the steady state period. The harmonic components of the two modulation methods are compared in Figure 8. It is clearly show that the SVPWM method has lower THD in the output current waveform. Figure 7 also shows the magnitude of the harmonics in the percentage of the fundamental.

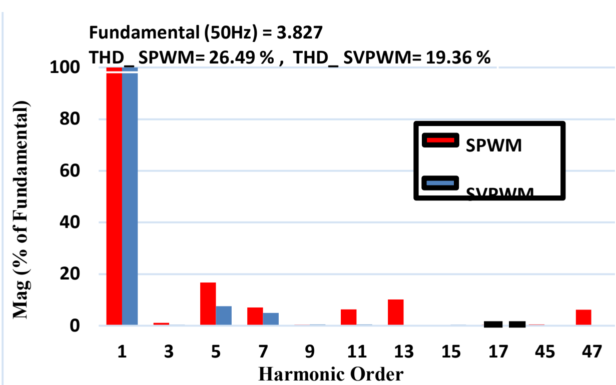

Figure 8. THD of the synchronverter current using both modulation methods.

The first forty-seven orders of the harmonics are presented. The THD decreases to 19.36% using SVPWM. Using the SVPWM, fifth, eleventh, and thirteenth order harmonics are eliminated while they highly appear in case of SPWM. The seventh harmonic is decreased from about 6.5% using SPWM to 4.8% using SVPWM. Such enhancements are also shown at the frequencies around the forty seventh order, which decreases from 6% to around 2.2%. Based on these observations, a smaller and cheaper is required for the SVPWM method. Table 3 summarizes the previous discussion of Section 5.

5.4 Rate of Change of Frequency (RoCoF)

Following a severe disturbance in power systems results in a significant imbalance between the power generated and the power consumed, the ability of the power system to maintain steady frequency refers to frequency stability. This type of stability depends on the ability to maintain a balance between the power generated and the loads with the minimum unintentional load losses [35]. Frequency instability that may occur results in the form of sustained fluctuations which leading to tripping of generating units and load events. The time derivative of the power system frequency is known as the Rate of Change of Frequency (RoCoF) [36].

. This value is inversely proportional to system inertia, with larger inertia of the system, the smaller the instantaneous RoCoF when the disturbance occurs. The frequency nadir is defined as the minimum value of frequency reached during the transient period and it depends on the system inertia and the primary frequency response. Since the rate of frequency change is inversely proportional to the system inertia, the high integration of renewable sources increases the frequency fluctuations and reduces the overall system stability [37]. Dynamic stability of power grid is essential to keep its operation safe, secure, reliable, and resilient within the stability margins [38-39].

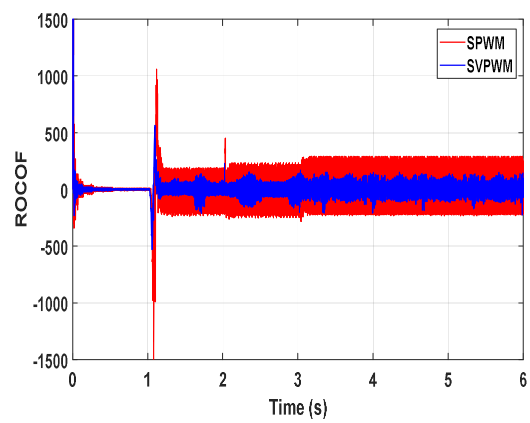

Figure 9. The rate of change of frequency using two modulation methods.

Figure 9 depicts the RoCoF for the two modulation techniques. From the figure, it is clear that the SVPWM is symmetrical around the time axis over the simulation time and has a lower ROCOF peak as compared to SPWM. Moreover, load variations have less effect on the RoCoF of SVPWM than SPWM.

TABLE 3. Comparative analysis of SVPWM Vs. SPWM for synchronverter**.**

Comparison Aspect	SVPWM Synchronverter	SPWM Synchronverter
Inertia	Better, the frequency response is slower.	Worst
Damping performance	Better achieving the damping behavior of SG.	Worst
Rate of Change of Frequency (ROCOF)	Lower, increases the system inertia.	Higher
Reactive power	Faster response, thus voltage supporting capability is enhanced.	Slower
THD	19.36%, THD is reduced by around 7%	26.49%

6 SVPWM Synchronverter Performance Evaluation

The SVPWM synchronverter shows better performance than SPWM synchronverter in many different terms. First, it mimics the behavior of synchronous generator. Second, it has high inertia response (lower frequency response). Thus, lower RoCof. Moreover, it gives more reliability to control the reactive power of the grid by supporting the voltage capability. Finally, it shows lower THD than the conventional SPWM synchronverter, which reduces the complexity of filter design.

7 Conclusion

This paper addresses the dynamic response of the synchronverter. The SPWM and SVPWM techniques were developed and used for comparison. The results confirm the efficacy of SVPWM. SVPWM outperforms SPWM for its ability to slow grid frequency. Therefore, SVPWM is more efficient in coping with the issues related the system instability like the substantial frequency deviations which may lead to load shedding or even a major blackout. The slow frequency response of the SVPWM Synchronverter contributes to enhancing the system inertia as low system inertia results in high rate of change of frequency (RoCoF). The results show that SVPWM method can mimic the damping performance of the synchronous generator better than the SPWM method. The current THD of SVPWM is reduced by 7% compared to SPWM, which reduces the cost and the size of the used filter.

In our future work, the requirements of self-synchronization methodology in addition to the phase locked loop (PLL) will be addressed and compared. High power synchronverter will be considered and studied, as its role mainly in supporting the grid frequency. Moreover, the efficiency analysis and enhancement of the SVPWM synchronverter will be discussed.

References:

[1] D. Ortiz-Villalba, C. Rahmann, R. Alvarez, C. A. Canizares, C. Strunk, Practical framework for frequency stability studies in power systems with renewable energy sources, *IEEE open access,* 2020, pp: 202286-202297.
[2] M. M. Almomani, A. Odienat, S. F. Al-Gharaibeh and K. Alawasa, The impact of wind generation on low frequency oscillation in power systems, 2021 *IEEE PES/IAS PowerAfrica,* 2021.
[3] A. Al-Odienat, K. Al-Maitah and B. Al-Khraisat, The enhancement of Frequency Stability of Low Inertia Interconnected Power System, *2021 IEEE PES/IAS PowerAfrica*, 2021.
[4] Q.-C. Zhong and G. Weiss, Synchronverters: Inverters that mimic synchronous generators, *IEEE transactions on industrial electronics*, 2010, Volume 58, pp. 1259–1267.
[5] L. He, Z. Shuai, X. Zhang, X. Liu, Z. Li, and Z. J. Shen, Transient characteristics of synchronverters subjected to asymmetric faults," *IEEE Transactions on Power Delivery, 2019,* Volume 34, pp. 1171–1183.
[6] R. V. Ferreira, S. M. Silva, H. M. Antunes, and G. Venkataramanan, Dynamic analysis of grid-connected droop-controlled converters and synchronverters, *Journal of Control, Automation and Electrical Systems*, 2019, Volume 30, pp. 741–753.
[7] J. Xu, T. Tang, and S. Xie, Research on low-order current harmonics rejections for grid-connected LCL-filtered inverters, *IET Power Electron*., 2014, Volume 7, pp. 1227–1234.
[8] I. Gabe, V. Montagner, H. Pinheiro, Design and implementation of a robust current controller for VSI connected to the grid through an LCL filter, *IEEE Trans. on Power Electronics*, 2009, Volume 24, pp. 1444–1452.
[9] S. Seo, Y. Cho, K. Lee, Design of an LCL-filter for space vector PWM in grid-connected 3-level

inverters system, IECON 2016, *42nd Annual Conference of the IEEE Industrial Electronics*, 2016.

[10] X. Wang, X. Ruan, S. Liu, C. Tse, Full feedforward of grid voltage for grid-connected inverter with LCL filter to suppress current distortion due to grid voltage harmonics, *IEEE Transactions on Power Electronics*, 2010, Volume 25, pp. 3119–3127.

[11] M. Liserre, F. Blaabjerg, S. Hansen, Design and control of an LCL-filter-based three-phase active rectifier, *IEEE Trans. on Industry Applications*, 2005, Volume 41, pp. 1281–1291.

[12] C. Nardi, C. M. O. Stein, E. G. Carati, J. P. Costa, R. Cardoso, A methodology of LCL filter design for grid-tied power converters, *13th Brazilian Power Electronics Conference and 1st southern Power Electronics Conference COPEB/SPEC*, 2015.

[13] A. S. Kale, A. V. Tamhane and A. A. Kalage, Comparative study of SPWM And SVPWM cascaded h-bridge multilevel inverter, *2017 International Conference on Intelligent Computing and Control (I2C2),* 2017.

[14] Saritha, A., T. Abhiran, and D. R. K. Sumanth, Space vector pulse width modulation for two level inverter, *International journal of professional engineering studies 6.3*, 2016.

[15] Rajlaxmi, E., Sasmita Behera, and Subrat Kumar Panda, Comparison of Inverter Control by SPWM and SVPWM Method in Standalone PV System, *2020 IEEE International Symposium on Sustainable Energy, Signal Processing and Cyber Security (iSSSC),* 2020.

[16] Kumar, K. Vinoth, et al. Simulation and comparison of SPWM and SVPWM control for three phase inverter, *ARPN journal of engineering and applied sciences,* 2010.

[17] Zhang, Liang, et al. An adaptative control strategy for interfacing converter of hybrid microgrid based on improved virtual synchronous generator, *IET Renewable Power Generation,* 2021.

[18] Zhang, Liang, et al. An integrated control algorithm of power distribution for islanded microgrid based on improved virtual synchronous generator. *IET Renewable Power Generation,* 2021.

[19] P. Tielens and D. Van Hertem, The relevance of inertia in power systems, *Renewable and Sustainable Energy Reviews*, 2016, Volume 55, pp. 999– 1009.

[20] Ying, Jie. Impact of inertia control on the structural loads of DFIG-based wind turbine connected to weak grid. *2020 12th IEEE PES Asia-Pacific Power and Energy Engineering Conference (APPEEC),* 2020.

[21] S. Dong and Y. C. Chen, Adjusting synchronverter dynamic response speed via damping correction loop, *IEEE Transactions on Energy Conversion*, 2016, Volume 32, pp. 608–619.

[22] X. Guo, Z. Lu, B. Wang, X. Sun, L. Wang, and J. M. Guerrero, Dynamic phasors-based modeling and stability analysis of droop-controlled inverters for microgrid applications, *IEEE Transactions on Smart Grid,* 2014, Volume 5, pp. 2980–2987, 2014.

[23] Z. Shuai, Y. Peng, J. M. Guerrero, Y. Li, and Z. J. Shen, Transient response analysis of inverter-based microgrids under unbalanced conditions using a dynamic phasor model, *IEEE Transactions on Industrial Electronics*, 2018, Volume 66, pp. 2868–2879.

[24] M. A. Al-Hitmi, S. Moinoddin, A. Iqbal, K. Rahman, and M. Meraj, Space vector vs. sinusoidal carrier-based pulse width modulation for a seven-phase voltage source inverter, *CPSS Transactions on Power Electronics and Applications*, 2019, Volume 4, pp. 230–243.

[25] P. S. Shete, R. G. Kanojiya, and N. S. Maurya, Performance of sinusoidal pulse width modulation based three phase inverter, *International Conference on Emerging Frontiers in Technology for Rural Area (EFITRA),* 2012.

[26] P. H. Zope, P. G. Bhangale, P. Sonare, and S. Suralkar, Design and implementation of carrier based sinusoidal pwm inverter, *International Journal of advanced research in electrical, electronics and instrumentation engineering,* 2012, Volume 1, pp. 230–236.

[27] V. Jayakumar, B. Chokkalingam and J. Munda, A Comprehensive review on space vector modulation techniques for neutral point clamped multi-level inverters, *IEEE Access*, 2021, Volume 9, pp. 112104-112144.

[28] B. P. McGrath, D. G. Holmes, and T. Lipo, Optimized space vector switching sequences for multilevel inverters, *IEEE Transactions on power electronics*, 2003, Volume 18, pp. 1293-1301.

[29] N. Prabaharan and K. Palanisamy, A comprehensive review on reduced switch multilevel inverter topologies, modulation techniques and applications, *Renewable and Sustainable Energy Reviews*, 2017, Volume 76, pp. 1248-1282.

[30] P. Tripura, Y. K. Babu, and Y. Tagore, Space vector pulse width modulation schemes for two-level voltage source inverter, *ACEEE Int. J. on control system and instrumentation*, 2011, Volume 2, pp. 34–38, 2011.

[31] L. Zhan, Y. Liu, and Y. Liu, A clarke transformation-based dft phasor and frequency algorithm for wide frequency range, *IEEE*

Transactions on Smart Grid, 2010, Volume 9, pp. 67–77.

[32] B. Dobrucky, M. Benova, and P. Spanik, Using complex conjugated magnitudes-and orthogonal park/clarke transformation methods of dc/ac/ac frequency converter, *Elektronika ir Elektrotechnika*, 2009, Volume 93, pp. 29–34.

[33] K. V. Kumar, P. A. Michael, J. P. John, and S. S. Kumar, Simulation and comparison of spwm and svpwm control for three phase inverter, *ARPN journal of engineering and applied sciences*, 2010, Volume 5, pp. 61–74.

[34] K. R. Vasudevan, V. K. Ramachandaramurthy, T. S. Babu, and A. Pouryekta, Synchronverter: A comprehensive review of modifications, stability assessment, applications and future perspectives, *IEEE Access*, 2020, Volume 8, pp. 131 565–131 589.

[35] K. Al-Maitah and A. Al-Odienat, Wide Area Protection Scheme for Active Distribution Network Aided µPMU, *IEEE PES/IAS PowerAfrica, 2020,* pp. 1-5, doi: 10.1109/PowerAfrica49420.2020.9219834.

[36] A. Al-Odienat and K. Al-Maitah, A modified Active Frequency Drift Method for Islanding Detection, *12th International Renewable Engineering Conference (IREC),* 2021, pp. 1-6, doi: 10.1109/IREC51415.2021.9427796.

[37] D. Stenclik, M. Richwine, N. Miller, L. Hong, The Role of Fast Frequency Response in Low Inertia Power Systems, *CIGRE: Paris*, France, 2018.

[38] A. Al-Odienat, Khaled Al-Maitah, A New Wide Area Protection Scheme Based on the Phase Angles of the Sequence Components, *Electric Power Components and Systems*, 2021, 49:4-5, 504-516, DOI: 10.1080/15325008.2021.1971335

[39] B. Wang, H. Sun, W. Li, Y. H. Yang, W. Wei, B. Zhao, S. Xu, Power system inertia estimation method based on maximum frequency deviation, *IET Renewable Power Generation, Wiley,* 2022, DOI: 10.1049/rpg2.12367

Contribution of individual authors to the creation of a scientific article (ghostwriting policy)

All authors are involved in simulation, writing, and editing this paper.